

Cosmology-independent Photon Mass Limits from Localized Fast Radio Bursts by using Artificial Neural Networks

Jing-Yu Ran,^{1,2,*} Bao Wang,^{1,2,*} and Jun-Jie Wei^{1,2,†}

¹*Purple Mountain Observatory, Chinese Academy of Sciences, Nanjing 210023, China*

²*School of Astronomy and Space Sciences, University of Science and Technology of China, Hefei 230026, China*

(Dated: April 29, 2024)

A hypothetical photon mass, m_γ , can produce a frequency-dependent vacuum dispersion of light, which leads to an additional time delay between photons with different frequencies when they propagate through a fixed distance. The dispersion measure–redshift measurements of fast radio bursts (FRBs) have been widely used to constrain the rest mass of the photon. However, all current studies analyzed the effect of the frequency-dependent dispersion for massive photons in the standard Λ CDM cosmological context. In order to alleviate the circularity problem induced by the presumption of a specific cosmological model based on the fundamental postulate of the masslessness of photons, here we employ a new model-independent smoothing technique, Artificial Neural Network (ANN), to reconstruct the Hubble parameter $H(z)$ function from 34 cosmic-chronometer measurements. By combining observations of 32 well-localized FRBs and the $H(z)$ function reconstructed by ANN, we obtain an upper limit of $m_\gamma \leq 3.5 \times 10^{-51}$ kg, or equivalently $m_\gamma \leq 2.0 \times 10^{-15}$ eV/c² ($m_\gamma \leq 6.5 \times 10^{-51}$ kg, or equivalently $m_\gamma \leq 3.6 \times 10^{-15}$ eV/c²) at the 1σ (2σ) confidence level. This is the first cosmology-independent photon mass limit derived from extragalactic sources.

PACS numbers: 14.70.Bh, 41.20.Jb, 52.25.Os, 95.85.Bh

I. INTRODUCTION

As a fundamental postulate of Maxwell’s electromagnetism and Einstein’s special relativity, the principle of the constancy of the speed of light implies the masslessness of photons, as elucidated by the particle-wave duality. This principle is also embraced within the framework of general relativity (GR). However, even a very minute photon mass, if existent, would necessitate new physical theories, such as the renowned de Broglie-Proca theory [1, 2], the model of massive photons as an explanation for dark energy [3], and other new ideas in the standard-model extension with massive photons [4]. Consequently, achieving precise constraints on the rest mass of photon, denoted as m_γ , remains an imperative.

Numerous experimental and observational constraints on m_γ have been derived from various effects resulting from the hypothetical nonzero photon mass. These include tests of Coulomb’s inverse square law [5], the Cavendish torsion balance [6, 7], gravitational deflection of electromagnetic waves [8], mechanical stability of magnetized gas in galaxies [9], magneto-hydrodynamic phenomena of the solar wind [10–13], Jupiter’s magnetic field [14], the spindown of a pulsar [15], among others. However, these constraints are contingent upon specific theories of massive photons and are thus dynamic tests in nature.

In contrast, a kinematic test based on the dispersion effect of the speed of light in vacuum is more inherently pure [16, 17]. The dispersion relation for massive photons is governed by

$$E^2 = p^2 c^2 + m_\gamma^2 c^4, \quad (1)$$

where p represents the momentum. The group velocity of a

photon with energy $E = h\nu$ can be expressed as

$$v = \frac{\partial E}{\partial p} = c \sqrt{1 - \frac{m_\gamma^2 c^4}{E^2}} \approx c \left(1 - \frac{1}{2} \frac{m_\gamma^2 c^4}{h^2 \nu^2} \right), \quad (2)$$

where h is the Planck constant and the last term is valid when $m_\gamma \ll h\nu/c^2 \approx 7 \times 10^{-42} (\nu/\text{GHz})$ kg. Eq. (2) suggests that if two photons with different frequencies are emitted simultaneously from the same source, they will be observed at different times due to their different velocities. Fast radio bursts (FRBs) provide an excellent celestial laboratory for detecting this dispersion effect, owing to their characteristics of (i) short time durations, (ii) long propagation distances, and (iii) low-frequency emissions.

Based on the vacuum dispersion method, several studies have used FRBs to put stringent upper limits on the photon mass [18–28]. Since FRBs originate at cosmological distances, the cosmic expansion rate $H(z)$ has to be considered in constraining the photon mass m_γ . In all previous studies, the required $H(z)$ information is calculated within the standard Λ CDM cosmological model. It should, however, be emphasized that Λ CDM is rooted in the framework of GR, which also embraces the postulate of the constancy of light speed. Thus, there is a circularity problem in constraining the photon mass. To address this problem, one has to determine the Hubble parameter $H(z)$ in a cosmology-independent way.

In this work, we propose a novel nonparametric approach, utilizing the Artificial Neural Network (ANN) technology, to reconstruct a smooth $H(z)$ function that best approximates the discrete $H(z)$ measurements. By combining observations of well-localized FRBs and the $H(z)$ function reconstructed by ANN, we aim to establish a cosmology-independent constraint on the rest mass of the photon. The paper is structured as follows. Section II introduces the theoretical framework and the observational data utilized for constraining the photon mass. Section III presents the cosmology-independent con-

*These authors contributed equally.

†jjwei@pmo.ac.cn

straints on the photon mass and other relevant parameters. Finally, a brief summary and discussions are given in Section IV.

II. ANALYSIS METHOD AND DATA

A. Theoretical framework

In our analysis, the observed time delay between different frequencies for FRBs is attributed to two main factors: (i) the propagation of photons through the plasma distributed between the source of the FRB and the observer, and (ii) the non-zero rest mass of the photon.

- Due to the interaction between the plasma and electromagnetic waves, photons with higher frequency ν_h travel faster than those with lower frequency ν_l , resulting in a dispersion effect. The time delay Δt_{DM} between photons of different frequencies caused by this dispersion effect can be described as [29, 30]

$$\begin{aligned} \Delta t_{\text{DM}} &= \int \frac{v_p^2}{2c} (\nu_l^{-2} - \nu_h^{-2}) dl \\ &= \frac{e^2}{8\pi^2 m_e \epsilon_0 c} (\nu_l^{-2} - \nu_h^{-2}) \text{DM}_{\text{astro}}, \end{aligned} \quad (3)$$

where $\nu_p \equiv \sqrt{\frac{n_e e^2}{4\pi^2 m_e \epsilon_0}}$ is the plasma frequency with the number density of electrons n_e , the charge of an electron e , the mass of an electron m_e , and the permittivity of vacuum ϵ_0 . Here DM_{astro} is the dispersion measure (DM) contributed by the plasma, which is defined as the integral of the number density of electrons n_e along the line of propagation, given by $\text{DM}_{\text{astro}} \equiv \int n_e dl$.

For an extragalactic source, DM_{astro} can be primarily divided into four components: the contributions from the Milky Way's interstellar medium ($\text{DM}_{\text{ISM}}^{\text{MW}}$), the Galactic halo ($\text{DM}_{\text{halo}}^{\text{MW}}$), the intergalactic medium (IGM; DM_{IGM}), and the host galaxy (DM_{host}). Therefore, DM_{astro} is given by

$$\begin{aligned} \text{DM}_{\text{astro}} &= \text{DM}_{\text{ISM}}^{\text{MW}} + \text{DM}_{\text{halo}}^{\text{MW}} \\ &\quad + \text{DM}_{\text{IGM}} + \frac{\text{DM}_{\text{host},0}}{1+z}, \end{aligned} \quad (4)$$

where the factor $(1+z)$ converts the DM component of the host galaxy in the rest frame, denoted as $\text{DM}_{\text{host},0}$, to the observed value DM_{host} .

- According to Eq. (2), the time delay Δt_{m_γ} between massive photons of high and low frequencies can be expressed as:

$$\Delta t_{m_\gamma} = \frac{1}{2} \left(\frac{m_\gamma c^2}{h} \right)^2 (\nu_l^{-2} - \nu_h^{-2}) H_\gamma(z), \quad (5)$$

where $H_\gamma(z)$ is a newly defined function related to redshift,

$$H_\gamma(z) = \int_0^z \frac{(1+z')^{-2}}{H(z')} dz', \quad (6)$$

where $H(z)$ is the Hubble parameter at redshift z . Note that here $H_\gamma(z)$ differs from the dimensionless redshift function that defined in previous works, and it is in units of $[\text{km s}^{-1} \text{Mpc}^{-1}]^{-1}$.

In our analysis, the total observed time delay is

$$\Delta t_{\text{obs}} = \Delta t_{\text{DM}} + \Delta t_{m_\gamma}. \quad (7)$$

Observationally, the time delay of all FRBs exhibits a frequency dependence of ν^{-2} , while both Δt_{DM} and Δt_{m_γ} follow a ν^{-2} behavior. Hence, it is natural for us to analogously define the equivalent DM arising from the massive photons as [31]

$$\text{DM}_\gamma(z) \equiv \frac{4\pi^2 m_e \epsilon_0 c^5}{h^2 e^2} H_\gamma(z) m_\gamma^2. \quad (8)$$

Thus, the observed DM obtained from fitting the ν^{-2} behavior in the total frequency-dependent time delay, can be written as:

$$\text{DM}_{\text{obs}} = \text{DM}_{\text{astro}} + \text{DM}_\gamma. \quad (9)$$

Once we are able to properly estimate the value of each DM term in Eq. (4), DM_γ can then be effectively extracted from DM_{obs} , thereby providing an upper limit on the photon mass m_γ .

The $\text{DM}_{\text{ISM}}^{\text{MW}}$ term arising from the ionizing medium around our galaxy is well modeled by some galactic electron distribution models. Here we adopt the NE2001 model [32] for its wide application. The value of $\text{DM}_{\text{halo}}^{\text{MW}}$ is challenging to estimate accurately, but it has been expected to lie within the range of $50 - 80 \text{ pc cm}^{-3}$ [33, 34]. Here, we conservatively adopt a Gaussian prior of $\text{DM}_{\text{halo}}^{\text{MW}} = 65 \pm 15 \text{ pc cm}^{-3}$ [27, 35].

The DM due to the IGM, DM_{IGM} , depends on the cosmological model and is largely influenced by the number of halos intersected along the propagation path. Due to density perturbations on large-scale structures, it is challenging to calculate the precise value of DM_{IGM} for individual FRBs. Instead, we typically calculate the average value of DM_{IGM} using [36]

$$\langle \text{DM}_{\text{IGM}}(z) \rangle = \frac{21c\Omega_b H_0^2 f_{\text{IGM}}}{64\pi G m_p} H_e(z), \quad (10)$$

where Ω_b is the baryon density parameter at the present day, H_0 is the Hubble constant, $f_{\text{IGM}} \approx 0.83$ is the fraction of baryon in the IGM [37], G is the gravitational constant, and m_p is the mass of proton. The redshift-dependent function $H_e(z)$ (in units of $[\text{km s}^{-1} \text{Mpc}^{-1}]^{-1}$) is defined by

$$H_e(z) \equiv \int_0^z \frac{(1+z')}{H(z')} dz'. \quad (11)$$

However, the actual value of DM_{IGM} may deviate from the average due to the inhomogeneity of IGM. To account for this

variability, we employ a one-parameter model to simulate the probability distribution of DM_{IGM} [24, 38, 39], which is given by

$$P_{\text{IGM}}(DM_{\text{IGM}}|z) = A\Delta^{-\beta} \exp\left[-\frac{(\Delta^{-\alpha} - C_0)^2}{2\alpha^2 s^2}\right], \quad (12)$$

where $\Delta \equiv DM_{\text{IGM}} / \langle DM_{\text{IGM}} \rangle > 0$, A is a normalization constant to ensure the integral of $P_{\text{IGM}}(DM_{\text{IGM}}|z)$ to be unity, C_0 is chosen to satisfy $\langle \Delta \rangle = 1$, and $\alpha = \beta = 3$ [39]. The fractional standard deviation of DM_{IGM} is approximated as $s = Fz^{-0.5}$, where F is the free parameter that quantifies the strength of baryon feedback [39]. Both semi-analytic models and numerical simulations of the IGM and galaxy halos showed that the probability distribution of DM_{IGM} can be well fitted by the quasi-Gaussian form (i.e., Eq. 12) [39, 40]. Therefore, this analytic form is adopted in our analysis.

The DM_{host} term is contributed by the source environment and the interstellar medium of the host galaxy, implying that the value of DM_{host} may vary significantly across different sources. To model this variability, we adopt a log-normal distribution for the probability density function of DM_{host} with the expression as [39]

$$P_{\text{host}}(DM_{\text{host}}|\mu, \sigma_{\text{host}}) = \frac{1}{\sqrt{2\pi}DM_{\text{host}}\sigma_{\text{host}}} \times \exp\left[-\frac{(\ln DM_{\text{host}} - \mu)^2}{2\sigma_{\text{host}}^2}\right], \quad (13)$$

where μ and σ_{host} are free parameters which are used to estimate the mean and standard deviation of $\ln DM_{\text{host}}$, respectively.

With the analyses stated above, we formulate the joint likelihood function for a sample of localized FRBs as

$$\mathcal{L} = \prod_{i=1}^N P_i(DM_{E,i}|z_i), \quad (14)$$

where N is the number of FRBs and $P_i(DM_{E,i}|z_i)$ denotes the likelihood for the i -th FRB with the corrected observable DM as

$$\begin{aligned} DM_E &\equiv DM_{\text{obs}} - DM_{\text{halo}}^{\text{MW}} - DM_{\text{ISM}}^{\text{MW}} \\ &= DM_{\text{IGM}} + DM_{\text{host}} + DM_{\gamma}. \end{aligned} \quad (15)$$

For a certain FRB at the redshift of z_i , we can estimate the probability distribution of DM_E with the combination of Eqs. (12), (13), and (15), which gives the expression as

$$\begin{aligned} P(DM_E|z_i) &= \int_0^{DM_E - DM_{\gamma}} P_{\text{host}}(DM_{\text{host}}|\mu, \sigma_{\text{host}}) \\ &\times P_{\text{IGM}}(DM_E - DM_{\text{host}} - DM_{\gamma}|z_i) dDM_{\text{host}}. \end{aligned} \quad (16)$$

Note that by Eq. (8), DM_{γ} is a constant at a given z_i . Denoting $P_X(X)$, $P_Y(Y)$, and $P_Z(Z)$ as the probability density functions of random variables X , Y , and Z , respectively. The equality $P_Z(Z) = \int_0^Z P_X(X)P_Y(Z-X)dX$ holds for every non-negative independent random variables X , Y , and Z , such that

$Z = X + Y$. As DM_{IGM} and DM_{host} are non-negative independent random variables, by setting $Z = DM_E - DM_{\gamma}$, $X = DM_{\text{host}}$, and $Y = DM_{\text{IGM}}$, it is easy to derive Eq. (16).

By maximizing the likelihood function \mathcal{L} , we can place constraints on the parameters in our model, including the rest mass of the photon m_{γ} . Nevertheless, there are two redshift-dependent functions, $H_{\gamma}(z)$ and $H_e(z)$ (see Eqs. 6 and 11), to be determined. In previous works [18–27], the conventional approach is to adopt the flat Λ CDM cosmological model and replace the denominator $H(z)$ with $H_0[\Omega_m(1+z)^3 + \Omega_{\Lambda}]^{1/2}$. Subsequently, $H_{\gamma}(z)$ and $H_e(z)$ are calculated by treating the cosmological parameters Ω_m and Ω_{Λ} as fixed values. However, it is crucial to note that the Λ CDM model is established within the framework of Einstein's theory of GR, which is derived from one of the fundamental postulates—the masslessness of photons. Consequently, adopting this model introduces a logical circularity problem in constraining the rest mass of the photon. To circumvent this issue, it is necessary to employ a cosmology-independent method to describe the relation between the Hubble parameter $H(z)$ and redshift z .

B. Artificial Neural Network

Gaussian Process (GP) is a widely-used approach for studying cosmology in a model-independent manner. This method assumes that the reconstructed value at a given point follows a Gaussian distribution, and the relationship between function values at different points is characterized by a selected covariance function [41]. Besides, the reconstructed function of $H(z)$ from GP tends to underestimate errors and is significantly influenced by the prior of the Hubble constant H_0 [42, 43]. In contrast, ANN, inspired by biological neural networks, is a mathematical model primarily used to discover intricate relationships between input and output data. The reconstructed function based on ANN makes no assumptions about the observational data and is entirely data-driven without parameterization of the function. Recently, Ref. [44] developed a public code called ReFANN¹ for reconstructing functions from data using ANN. Their reconstructed $H(z)$ function showed no sensitivity to the setting of H_0 , indicating that reconstructing $H(z)$ from observational data using ANN may be more reliable than using GP. To make a cosmology-independent determination of $H(z)$, in this work we will reconstruct a smooth curve of $H(z)$ from 34 model-independent measurements of $H(z)$ using ReFANN.

The first step in using ReFANN to reconstruct a function from data is to find the best parameter configuration for the model used to train the data. Following the approach of Ref. [44], we determine the optimal network model by mini-

¹ <https://github.com/Guo-Jian-Wang/refann>

mizing the *risk* [45]:

$$\begin{aligned} \text{risk} &= \sum_{i=1}^N \text{Bias}_i^2 + \sum_{i=1}^N \text{Variance}_i \\ &= \sum_{i=1}^N [H(z_i) - \bar{H}(z_i)]^2 + \sum_{i=1}^N \sigma_{H(z_i)}^2, \end{aligned} \quad (17)$$

where N is the number of sample $H(z)$ and $\bar{H}(z_i)$ is the fiducial value of $H(z)$ at redshift z_i . For our purposes, we only consider the number of hidden layers and neurons in the hidden layer. Through experimentation, we determined that the optimal model configuration involves a single hidden layer with 4096 neurons. Additionally, to reduce sensitivity to initialization and stabilize the distribution among variables, we employ batch normalization [46] in our network model, with the batch size set to half of the number of $H(z)$ data points. We also use the Exponential Linear Unit [47] as the activation function, with the hyperparameter α set to be 1. Furthermore, we utilize the Adam optimizer [48] to update the network parameters in each iteration of the training process.

Subsequently, we train this optimal network model with the observational $H(z)$ data. This training process provides us with a predicted value of $H(z_i)$ and its associated error $\sigma_{H(z_i)}$ at a given redshift z_i . This predicted function represents an approximate reconstruction of $H(z)$ based on the ANN model trained with observational data.

C. Hubble parameter $H(z)$ Data

The Hubble parameter $H(z)$, which quantifies the expansion rate of the universe as a function of time (or equivalently redshift), has been extensively used for exploring the nature of dark energy and testing modified theories of gravity. $H(z)$ can be measured using two main methods. One approach is based on the detection of the radial baryon acoustic oscillation features [60–62]. However, this method relies on assumptions about the underlying cosmological model, typically the Λ CDM model. Therefore, in our analysis, we focus exclusively on $H(z)$ measurements obtained using another method, namely the cosmic chronometers (CC) method [63]. This method is model-independent as it relies on minimal assumptions, primarily the use of a Friedmann-Lemaître-Robertson-Walker metric. In this method, by combining the definition of $H(z) \equiv \dot{a}/a$ and the relation between the scale factor $a(t)$ and redshift, $1+z = 1/a(t)$, $H(z)$ can be rewritten as

$$H(z) = -\frac{1}{1+z} \frac{dz}{dt}. \quad (18)$$

This means that one can achieve a model-independent determination of $H(z)$ by calculating the differential age of the universe using passively evolving galaxies at various redshifts. We compile the latest 34 CC $H(z)$ measurements in Table I, covering the redshift range of $0.07 < z < 1.965$.

Having obtained the dataset of $H(z)$, we adopt ANN to reconstruct the $H(z)$ function within the redshift range of $0 < z < 2$, and the results are shown in Fig. 1. The black

TABLE I: 34 $H(z)$ measurements obtained with the CC method.

z	$H(z)$ (km s ⁻¹ Mpc ⁻¹)	σ (km s ⁻¹ Mpc ⁻¹)	Refs.
0.09	69	12	[49]
0.17	83	8	
0.27	77	14	
0.4	95	17	
0.9	117	23	[50]
1.3	168	17	
1.43	177	18	
1.53	140	14	
1.75	202	40	
0.48	97	62	[51]
0.88	90	40	
0.1791	75	4	
0.1993	75	5	
0.3519	83	14	
0.5929	104	13	[52]
0.6797	92	8	
0.7812	105	12	
0.8754	125	17	
1.037	154	20	
0.07	69	19.6	
0.12	68.2	26.2	[53]
0.2	72.9	29.6	
0.28	88.8	36.6	
1.363	160	33.6	[54]
1.965	186.5	50.4	
0.3802	83	13.5	
0.4004	77	10.2	
0.4247	87.1	11.2	[55]
0.4497	92.8	12.9	
0.4783	80.9	9	
0.47	89	49.6	[56]
0.75	98.8	33.6	[57]
0.8	113.1	25.22	[58]
1.26	135	65	[59]

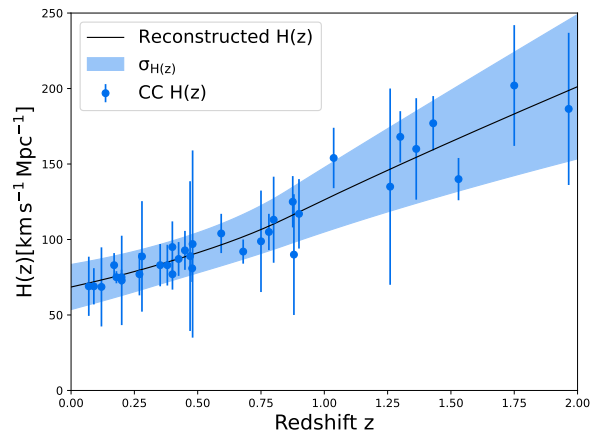


FIG. 1: Reconstruction of the Hubble parameter $H(z)$ from 34 CC $H(z)$ measurements using ANN. The shaded area corresponds to the 1σ confidence region of the reconstruction. The blue dots with error bars depict the observational $H(z)$ data.

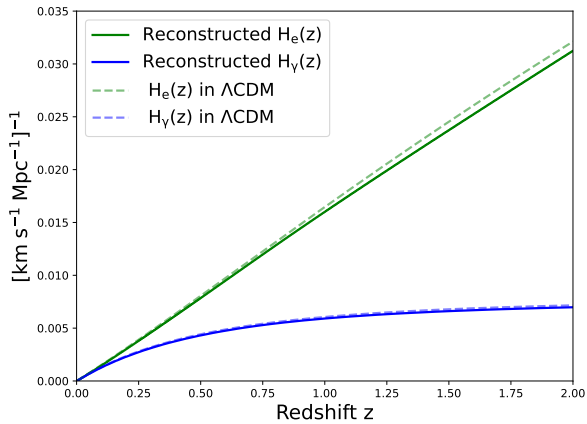


FIG. 2: The redshift dependence of the reconstructed $H_\gamma(z)$ and $H_e(z)$ functions (solid lines). The corresponding theoretical curves (dashed lines) derived from the flat Λ CDM model with $\Omega_m = 0.315$ and $H_0 = 67.4 \text{ km s}^{-1} \text{ Mpc}^{-1}$ are also shown.

line represents the best fit, and the blue shaded area indicates the 1σ confidence region of the reconstructed function. The redshift-dependent $H_\gamma(z)$ and $H_e(z)$ functions can then be derived by integrating the reconstructed $H(z)$ function with respect to redshift. As shown in Fig. 2, the reconstructed $H_\gamma(z)$ and $H_e(z)$ functions exhibit significant differences in behavior as a function of redshift z . Such distinctions are crucial for breaking parameter degeneracy and enhancing sensitivity in testing the photon mass when a few redshift measurements of FRBs are available [19–21, 23, 64]. For comparison, we also plot $H_\gamma(z)$ and $H_e(z)$ functions within the framework of the flat Λ CDM model using Planck 2018 parameters ($\Omega_m = 0.315$ and $H_0 = 67.4 \text{ km s}^{-1} \text{ Mpc}^{-1}$) [65]. The corresponding theoretical curves are presented in Fig. 2 as dashed lines. It is evident that the reconstructions of $H_\gamma(z)$ and $H_e(z)$ are roughly consistent with the predictions of the standard Λ CDM model, implying that the ANN method can offer a reliable reconstructed function from the observational data.

D. Fast Radio Burst Data

Expanding upon the sample of 23 localized FRBs utilized in Ref. [27], we incorporate 9 new localized FRBs recently detected by the 110-antenna Deep Synoptic Array [66]. Note that another two new FRBs with redshift measurements, FRB 20220319D and FRB 20220914A, are not included in our sample. FRB 20220319D exhibits an observed DM_{obs} value of $110.98 \text{ pc cm}^{-3}$, while the $\text{DM}_{\text{ISM}}^{\text{MW}}$ value calculated using the NE2001 model stands at 133.3 pc cm^{-3} , leading to its exclusion from our analysis. Furthermore, FRB 20220914A is omitted due to its notable deviation from the expected $\text{DM}_{\text{IGM}}-z$ relation outlined in Eq. (10). The total 32 localized FRBs, including their respective redshifts, DM_{obs} , and $\text{DM}_{\text{ISM}}^{\text{MW}}$, are provided in Table II.

TABLE II: Properties of 32 localized FRBs.

Name	z	DM_{obs} (pc cm^{-3})	$\text{DM}_{\text{ISM}}^{\text{MW}}$ (pc cm^{-3})	Refs.
FRB 20121102	0.19273	557	188.0	[67]
FRB 20180301	0.3304	536	152.0	[68]
FRB 20180916	0.0337	348.76	200.0	[69]
FRB 20180924	0.3214	361.42	40.5	[70]
FRB 20181112	0.4755	589.27	102.0	[71]
FRB 20190102	0.291	363.6	57.3	[72]
FRB 20190523	0.66	760.8	37.0	[73]
FRB 20190608	0.1178	338.7	37.2	[74]
FRB 20190611	0.378	321.4	57.83	[75]
FRB 20190614	0.6	959.2	83.5	[76]
FRB 20190711	0.522	593.1	56.4	[75]
FRB 20190714	0.2365	504	38.0	[75]
FRB 20191001	0.234	506.92	44.7	[75]
FRB 20191228	0.2432	297.5	33.0	[68]
FRB 20200430	0.16	380.1	27.0	[75]
FRB 20200906	0.3688	577.8	36.0	[68]
FRB 20201124	0.098	413.52	123.2	[77]
FRB 20210117	0.2145	730	34.4	[78]
FRB 20210320	0.27970	384.8	42	[78]
FRB 20210807	0.12927	251.9	121.2	[78]
FRB 20211127	0.0469	234.83	42.5	[78]
FRB 20211212	0.0715	206	27.1	[78]
FRB 20220207C	0.043040	262.38	79.3	[66]
FRB 20220307B	0.28123	499.27	135.7	[66]
FRB 20220310F	0.477958	462.24	45.4	[66]
FRB 20220418A	0.622000	623.25	37.6	[66]
FRB 20220506D	0.30039	396.97	89.1	[66]
FRB 20220509G	0.089400	269.53	55.2	[66]
FRB 20220610A	1.016	1457.624	31	[79]
FRB 20220825A	0.241397	651.24	79.7	[66]
FRB 20220920A	0.158239	314.99	40.3	[66]
FRB 20221012A	0.284669	441.08	54.4	[66]

III. RESULTS

We explore the posterior probability distributions of the free parameters by maximizing the joint likelihood function \mathcal{L} (Eq. 14) using emcee, an affine-invariant Markov Chain Monte Carlo (MCMC) ensemble sampler implemented in Python [80]. The free parameters of our model now include the baryon density parameter $\Omega_b h_0^2$ (where $h_0 \equiv H_0/(100 \text{ km s}^{-1} \text{ Mpc}^{-1})$), the DM contribution from the Milky Way’s halo $\text{DM}_{\text{halo}}^{\text{MW}}$, the parameters related to the probability distributions for DM_{IGM} and DM_{host} (i.e., F , μ , and σ_{host}), and the photon mass m_γ . In our MCMC analysis, we set uniform priors on $\Omega_b h_0^2 \in [0.01, 1]$, $F \in [0.01, 0.5]$, $e^\mu \in [20, 200]$ pc cm^{-3} , $\sigma_{\text{host}} \in [0.2, 2]$, and $m_\gamma \in [0, 10^{-49}] \text{ kg}$. For $\text{DM}_{\text{halo}}^{\text{MW}}$, we set a Gaussian prior, $\text{DM}_{\text{halo}}^{\text{MW}} = 65 \pm 15 \text{ pc cm}^{-3}$, within the wide 3σ range of $[20, 110] \text{ pc cm}^{-3}$. To incorporate the error of the ANN reconstruction into our analysis, at each MCMC step, we sample the Hubble rate $\tilde{H}(z)$ function according to the Gaussian distribution $\tilde{H}(z) = \mathcal{N}(H(z), \sigma_{H(z)})$ with mean $H(z)$ and standard deviation $\sigma_{H(z)}$. Here $H(z)$ is the best-fit function reconstructed by ANN and $\sigma_{H(z)}$ is the 1σ error of the reconstructed $H(z)$ function.

The 1σ constraint results for these six parameters are summarized in Table III. For the photon mass m_γ , both the 1σ and 2σ upper limits are presented. Posterior distributions and $1 - 2\sigma$ confidence regions for these parameters are displayed in Fig. 3. Notably, the constraints on m_γ are determined as

$$m_\gamma \leq 3.5 \times 10^{-51} \text{ kg} \approx 2.0 \times 10^{-15} \text{ eV}/c^2 \quad (19)$$

and

$$m_\gamma \leq 6.5 \times 10^{-51} \text{ kg} \approx 3.6 \times 10^{-15} \text{ eV}/c^2 \quad (20)$$

at the 1σ and 2σ confidence level, respectively. Meanwhile, we find that the baryon density parameter is optimized to be $\Omega_b h_0^2 = 0.030^{+0.006}_{-0.007}$, which is compatible with the value inferred from Planck 2018 ($\Omega_b h_0^2 = 0.0224 \pm 0.0001$) at the 1.2σ confidence level [65].

To investigate the impact of the prior assumption of $\text{DM}_{\text{halo}}^{\text{MW}}$ on our results, we also perform a parallel comparative analysis of the FRB data using a flat prior on $\text{DM}_{\text{halo}}^{\text{MW}} \in [20, 110]$ pc cm⁻³. The corresponding resulting constraints on all parameters are also reported in Table III. Comparing these inferred parameters with those obtained from the Gaussian prior (see line 1 in Table III), it is clear that, except for the best-fit value of $\text{DM}_{\text{halo}}^{\text{MW}}$, the prior assumption of $\text{DM}_{\text{halo}}^{\text{MW}}$ only has a minimal influence on our results.

IV. DISCUSSION AND CONCLUSIONS

As a matter of fact, it is impossible to prove experimentally that the rest mass of a photon is strictly zero. According to the uncertainty principle of quantum mechanics, the ultimately measurable order of magnitude for the photon mass is $m_\gamma \approx \hbar/(\Delta t c^2) \approx 10^{-69}$ kg, where \hbar is the reduced Planck constant and $\Delta t \approx 10^{10}$ years is the age of our universe. However, due to the immense importance of Maxwell's theory and Einstein's theory of relativity, it is still intellectually stimulating and scientifically significant to approach this ultimate limit by various experiments.

FRBs provide the current best celestial laboratory to test the photon mass m_γ via the dispersion method. Constraining m_γ with cosmological FRBs, however, one has to know the cosmic expansion rate $H(z)$. In all previous studies, the required $H(z)$ information is estimated within the standard Λ CDM cosmological model. Such $H(z)$ estimations would involve a circularity problem in constraining m_γ , since Λ CDM

itself is built on the framework of GR and GR embraces the postulate of the constancy of light speed. In this work, aiming to overcome the circularity problem, we have employed an ANN technology to reconstruct a cosmology-independent $H(z)$ function from the discrete CC $H(z)$ data.

By combining the DM- z measurements of 32 localized FRBs with the reconstructed $H(z)$ function from 34 CC $H(z)$ data, we have placed the first cosmology-independent photon mass limit. Our results show that the 1σ and 2σ confidence-level upper limits on the photon mass are $m_\gamma \leq 3.5 \times 10^{-51}$ kg (or equivalently $m_\gamma \leq 2.0 \times 10^{-15}$ eV/ c^2) and $m_\gamma \leq 6.5 \times 10^{-51}$ kg (or equivalently $m_\gamma \leq 3.6 \times 10^{-15}$ eV/ c^2), respectively. Previously, under the assumption of fiducial Λ CDM cosmology, Ref. [24] obtained an upper limit of $m_\gamma \leq 3.1 \times 10^{-51}$ kg at the 1σ confidence level by using a catalog of 129 FRBs (most of them without redshift measurement, and the observed DM_{obs} values were used to estimate the pseudo redshifts). Ref. [26] obtained $m_\gamma \leq 4.8 \times 10^{-51}$ kg (1σ) by analyzing a sample of 17 localized FRBs in the flat Λ CDM model. Ref. [27] obtained $m_\gamma \leq 3.8 \times 10^{-51}$ kg (1σ) for flat Λ CDM using a sample of 23 localized FRBs. Despite not assuming a specific cosmological model, the precision of our constraint from 32 localized FRBs is comparable to these previous results. Most importantly, this highlights the validity of our approach and suggests that as the number of CC $H(z)$ measurements increases, we can expect even more reliable model-independent tests of the photon mass.

Acknowledgments

We are grateful to the anonymous referees for their helpful comments. This work is partially supported by the National SKA Program of China (2022SKA0130100), the National Natural Science Foundation of China (grant Nos. 12373053, 12321003, and 12041306), the Key Research Program of Frontier Sciences (grant No. ZDBS-LY-7014) of Chinese Academy of Sciences, International Partnership Program of Chinese Academy of Sciences for Grand Challenges (114332KYSB20210018), the CAS Project for Young Scientists in Basic Research (grant No. YSBR-063), the CAS Organizational Scientific Research Platform for National Major Scientific and Technological Infrastructure: Cosmic Transients with FAST, and the Natural Science Foundation of Jiangsu Province (grant No. BK20221562).

-
- [1] L. De Broglie, *J. Phys. Radium* **3**, 422 (1922).
[2] A. Proca, *J. Phys. Radium* **7**, 347 (1936).
[3] S. Kouwn, P. Oh, and C.-G. Park, *Phys. Rev. D* **93**, 083012 (2016), arXiv:1512.00541 [astro-ph.CO].
[4] A. D. A. M. Spallicci, J. A. Helayël-Neto, M. López-Corredoira, and S. Capozziello, *European Physical Journal C* **81**, 4 (2021), arXiv:2011.12608 [astro-ph.CO].
[5] E. R. Williams, J. E. Faller, and H. A. Hill, *Phys. Rev. Lett.* **26**, 721 (1971).
[6] R. Lakes, *Phys. Rev. Lett.* **80**, 1826 (1998).
[7] J. Luo, L.-C. Tu, Z.-K. Hu, and E.-J. Luan, *Phys. Rev. Lett.* **90**, 081801 (2003).
[8] D. D. Lowenthal, *Phys. Rev. D* **8**, 2349 (1973).
[9] G. V. Chibisov, *Uspekhi Fizicheskikh Nauk* **119**, 551 (1976).
[10] D. D. Ryutov, *Plasma Physics and Controlled Fusion* **39**, A73 (1997).

TABLE III: The 1σ constraints for all parameters with different priors on $DM_{\text{halo}}^{\text{MW}}$. Both the 1σ and 2σ upper limits for the photon mass m_γ are provided.

Priors of $DM_{\text{halo}}^{\text{MW}}$	$\Omega_b h_0^2$	F	$DM_{\text{halo}}^{\text{MW}}$ (pc cm^{-3})	μ	σ_{host}	m_γ (10^{-51} kg)
Gaussian prior	$0.030^{+0.006}_{-0.007}$	≥ 0.449	39^{+10}_{-10}	$4.02^{+0.46}_{-0.29}$	$1.01^{+0.22}_{-0.37}$	≤ 3.5 (≤ 6.5)
Flat prior	$0.031^{+0.006}_{-0.006}$	≥ 0.451	≤ 32	$4.07^{+0.48}_{-0.30}$	$0.99^{+0.21}_{-0.37}$	≤ 3.8 (≤ 7.2)

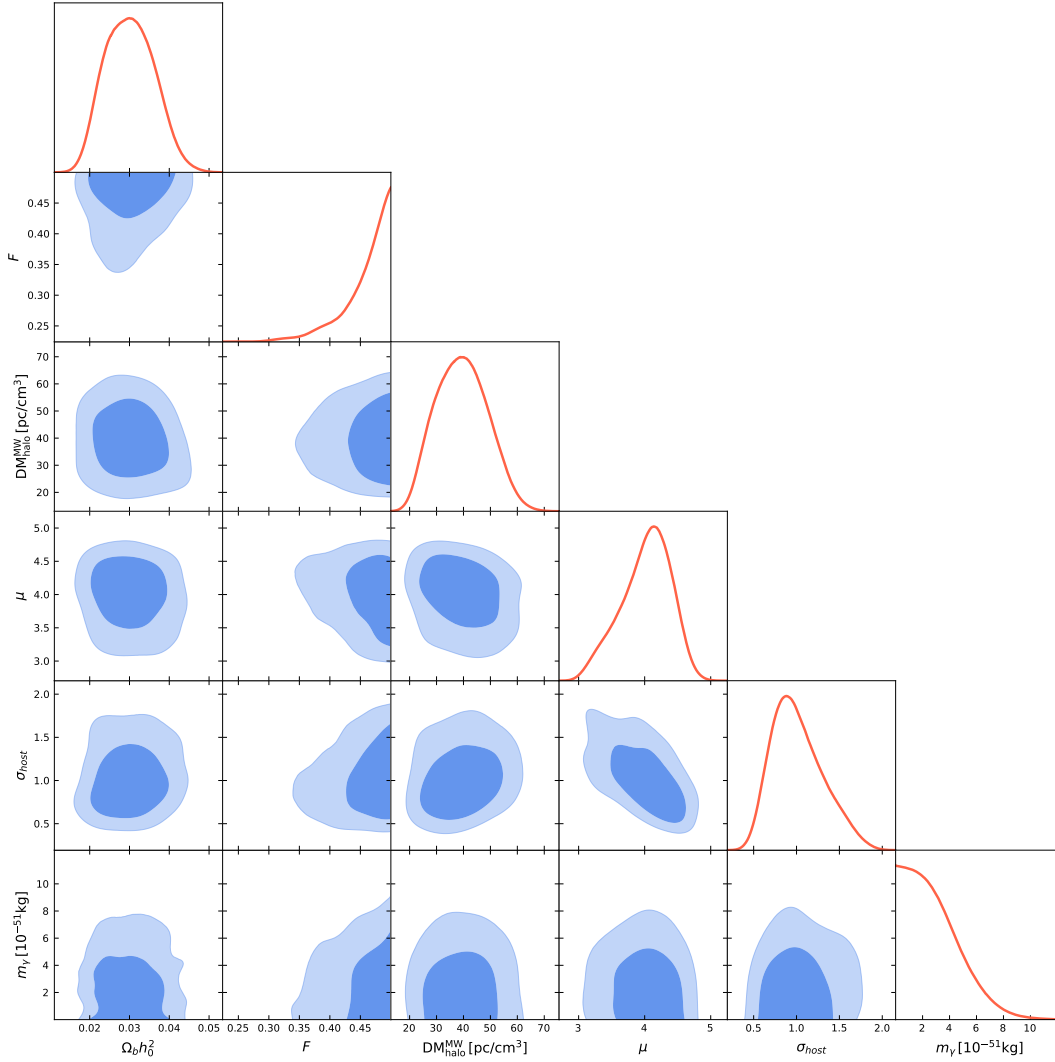


FIG. 3: Plots of 1D marginalized probability distributions and 2D 1 – 2 σ confidence contours for the parameters $\Omega_b h_0^2$, F , $DM_{\text{halo}}^{\text{MW}}$, μ , σ_{host} , and m_γ , constrained by 32 localized FRBs.

- [11] D. D. Ryutov, *Plasma Physics and Controlled Fusion* **49**, B429 (2007).
- [12] L.-X. Liu and C.-G. Shao, *Chinese Physics Letters* **29**, 111401 (2012).
- [13] A. Retinò, A. D. A. M. Spallicci, and A. Vaivads, *Astroparticle Physics* **82**, 49 (2016), arXiv:1302.6168 [hep-ph].
- [14] J. Davis, L., A. S. Goldhaber, and M. M. Nieto, *Phys. Rev. Lett.* **35**, 1402 (1975).
- [15] Y.-P. Yang and B. Zhang, *Astrophys. J.* **842**, 23 (2017), arXiv:1701.03034 [astro-ph.HE].
- [16] L.-C. Tu, H.-L. Ye, and J. Luo, *Chinese Physics Letters* **22**, 3057 (2005).
- [17] L.-C. Tu, J. Luo, and G. T. Gillies, *Reports on Progress in Physics* **68**, 77 (2005).
- [18] X.-F. Wu, S.-B. Zhang, H. Gao, *et al.*, *Astrophys. J. Lett.* **822**, L15 (2016), arXiv:1602.07835 [astro-ph.HE].
- [19] L. Bonetti, J. Ellis, N. E. Mavromatos, *et al.*, *Physics Letters B* **757**, 548 (2016), arXiv:1602.09135 [astro-ph.HE].
- [20] L. Bonetti, J. Ellis, N. E. Mavromatos, *et al.*, *Physics Letters B* **768**, 326 (2017), arXiv:1701.03097 [astro-ph.HE].
- [21] L. Shao and B. Zhang, *Phys. Rev. D* **95**, 123010 (2017), arXiv:1705.01278 [hep-ph].

- [22] N. Xing, H. Gao, J.-J. Wei, *et al.*, *Astrophys. J. Lett.* **882**, L13 (2019), arXiv:1907.00583 [astro-ph.HE] .
- [23] J.-J. Wei and X.-F. Wu, *Research in Astronomy and Astrophysics* **20**, 206 (2020), arXiv:2006.09680 [astro-ph.HE] .
- [24] H. Wang, X. Miao, and L. Shao, *Physics Letters B* **820**, 136596 (2021), arXiv:2103.15299 [astro-ph.HE] .
- [25] C.-M. Chang, J.-J. Wei, S.-b. Zhang, and X.-F. Wu, *JCAP* **2023**, 010 (2023), arXiv:2207.00950 [astro-ph.HE] .
- [26] H.-N. Lin, L. Tang, and R. Zou, *Mon. Not. R. Astron. Soc.* **520**, 1324 (2023), arXiv:2301.12103 [gr-qc] .
- [27] B. Wang, J.-J. Wei, X.-F. Wu, and M. López-Corredoira, *JCAP* **2023**, 025 (2023), arXiv:2304.14784 [astro-ph.HE] .
- [28] Y.-B. Wang, X. Zhou, A. Kurban, and F.-Y. Wang, *Astrophys. J.* **965**, 38 (2024), arXiv:2403.06422 [astro-ph.HE] .
- [29] D. R. Lorimer and M. Kramer, *Handbook of Pulsar Astronomy* (2012).
- [30] M. J. Bentum, L. Bonetti, and A. D. Spallicci, *Advances in Space Research* **59**, 736 (2017).
- [31] L. Shao and B. Zhang, *Phys. Rev. D* **95**, 123010 (2017).
- [32] J. M. Cordes and T. J. W. Lazio, arXiv e-prints , astro-ph/0207156 (2002), arXiv:astro-ph/0207156 [astro-ph] .
- [33] J. X. Prochaska and Y. Zheng, *Mon. Not. R. Astron. Soc.* **485**, 648 (2019), arXiv:1901.11051 [astro-ph.GA] .
- [34] L. C. Keating and U.-L. Pen, *Mon. Not. R. Astron. Soc.* **496**, L106 (2020), arXiv:2001.11105 [astro-ph.GA] .
- [35] Q. Wu, G.-Q. Zhang, and F.-Y. Wang, *Mon. Not. R. Astron. Soc.* **515**, L1 (2022), arXiv:2108.00581 [astro-ph.CO] .
- [36] W. Deng and B. Zhang, *Astrophys. J. Lett.* **783**, L35 (2014), arXiv:1401.0059 [astro-ph.HE] .
- [37] M. Fukugita, C. J. Hogan, and P. J. E. Peebles, *Astrophys. J.* **503**, 518 (1998), arXiv:astro-ph/9712020 [astro-ph] .
- [38] J. Miralda-Escudé, M. Haehnelt, and M. J. Rees, *Astrophys. J.* **530**, 1 (2000), arXiv:astro-ph/9812306 [astro-ph] .
- [39] J. P. Macquart, J. X. Prochaska, M. McQuinn, *et al.*, *Nature (London)* **581**, 391 (2020), arXiv:2005.13161 [astro-ph.CO] .
- [40] M. McQuinn, *Astrophys. J. Lett.* **780**, L33 (2014), arXiv:1309.4451 [astro-ph.CO] .
- [41] M. Seikel, C. Clarkson, and M. Smith, *JCAP* **2012**, 036 (2012), arXiv:1204.2832 [astro-ph.CO] .
- [42] J.-J. Wei and X.-F. Wu, *Astrophys. J.* **838**, 160 (2017), arXiv:1611.00904 [astro-ph.CO] .
- [43] G.-J. Wang, J.-J. Wei, Z.-X. Li, *et al.*, *Astrophys. J.* **847**, 45 (2017), arXiv:1709.07258 [astro-ph.CO] .
- [44] G.-J. Wang, X.-J. Ma, S.-Y. Li, and J.-Q. Xia, *Astrophys. J. Suppl. Ser.* **246**, 13 (2020), arXiv:1910.03636 [astro-ph.CO] .
- [45] L. Wasserman, C. J. Miller, R. C. Nichol, *et al.*, arXiv e-prints , astro-ph/0112050 (2001), arXiv:astro-ph/0112050 [astro-ph] .
- [46] S. Ioffe and C. Szegedy, arXiv e-prints , arXiv:1502.03167 (2015), arXiv:1502.03167 [cs.LG] .
- [47] D.-A. Clevert, T. Unterthiner, and S. Hochreiter, arXiv e-prints , arXiv:1511.07289 (2015), arXiv:1511.07289 [cs.LG] .
- [48] D. P. Kingma and J. Ba, arXiv e-prints , arXiv:1412.6980 (2014), arXiv:1412.6980 [cs.LG] .
- [49] R. Jimenez, L. Verde, T. Treu, and D. Stern, *Astrophys. J.* **593**, 622 (2003), arXiv:astro-ph/0302560 [astro-ph] .
- [50] J. Simon, L. Verde, and R. Jimenez, *Phys. Rev. D* **71**, 123001 (2005), arXiv:astro-ph/0412269 [astro-ph] .
- [51] D. Stern, R. Jimenez, L. Verde, *et al.*, *JCAP* **2010**, 008 (2010), arXiv:0907.3149 [astro-ph.CO] .
- [52] M. Moresco, A. Cimatti, R. Jimenez, *et al.*, *JCAP* **2012**, 006 (2012), arXiv:1201.3609 [astro-ph.CO] .
- [53] C. Zhang, H. Zhang, S. Yuan, *et al.*, *Research in Astronomy and Astrophysics* **14**, 1221-1233 (2014), arXiv:1207.4541 [astro-ph.CO] .
- [54] M. Moresco, *Mon. Not. R. Astron. Soc.* **450**, L16 (2015), arXiv:1503.01116 [astro-ph.CO] .
- [55] M. Moresco, L. Pozzetti, A. Cimatti, *et al.*, *JCAP* **2016**, 014 (2016), arXiv:1601.01701 [astro-ph.CO] .
- [56] A. L. Ratsimbazafy, S. I. Loubser, S. M. Crawford, *et al.*, *Mon. Not. R. Astron. Soc.* **467**, 3239 (2017), arXiv:1702.00418 [astro-ph.CO] .
- [57] N. Borghi, M. Moresco, and A. Cimatti, *Astrophys. J. Lett.* **928**, L4 (2022), arXiv:2110.04304 [astro-ph.CO] .
- [58] K. Jiao, N. Borghi, M. Moresco, and T.-J. Zhang, *Astrophys. J. Suppl. Ser.* **265**, 48 (2023), arXiv:2205.05701 [astro-ph.CO] .
- [59] E. Tomasetti, M. Moresco, N. Borghi, *et al.*, *Astron. & Astrophys.* **679**, A96 (2023), arXiv:2305.16387 [astro-ph.CO] .
- [60] E. Gaztañaga, A. Cabré, and L. Hui, *Mon. Not. R. Astron. Soc.* **399**, 1663 (2009), arXiv:0807.3551 [astro-ph] .
- [61] C. Blake, S. Brough, M. Colless, *et al.*, *Mon. Not. R. Astron. Soc.* **425**, 405 (2012), arXiv:1204.3674 [astro-ph.CO] .
- [62] L. Samushia, B. A. Reid, M. White, *et al.*, *Mon. Not. R. Astron. Soc.* **429**, 1514 (2013), arXiv:1206.5309 [astro-ph.CO] .
- [63] R. Jimenez and A. Loeb, *Astrophys. J.* **573**, 37 (2002), arXiv:astro-ph/0106145 [astro-ph] .
- [64] M. J. Bentum, L. Bonetti, and A. D. A. M. Spallicci, *Advances in Space Research* **59**, 736 (2017), arXiv:1607.08820 [astro-ph.IM] .
- [65] Planck Collaboration *et al.*, *Astron. & Astrophys.* **641**, A6 (2020), arXiv:1807.06209 [astro-ph.CO] .
- [66] C. J. Law, K. Sharma, V. Ravi, *et al.*, arXiv e-prints , arXiv:2307.03344 (2023), arXiv:2307.03344 [astro-ph.HE] .
- [67] S. Chatterjee, C. J. Law, R. S. Wharton, *et al.*, *Nature (London)* **541**, 58 (2017), arXiv:1701.01098 [astro-ph.HE] .
- [68] S. Bhandari, K. E. Heintz, K. Aggarwal, *et al.*, *Astron. J.* **163**, 69 (2022), arXiv:2108.01282 [astro-ph.HE] .
- [69] B. Marcote, K. Nimmo, J. W. T. Hessels, *et al.*, *Nature (London)* **577**, 190 (2020), arXiv:2001.02222 [astro-ph.HE] .
- [70] K. W. Bannister, A. T. Deller, C. Phillips, *et al.*, *Science* **365**, 565 (2019), arXiv:1906.11476 [astro-ph.HE] .
- [71] J. X. Prochaska, J.-P. Macquart, M. McQuinn, *et al.*, *Science* **366**, 231 (2019), arXiv:1909.11681 [astro-ph.GA] .
- [72] S. Bhandari, E. M. Sadler, J. X. Prochaska, *et al.*, *Astrophys. J. Lett.* **895**, L37 (2020), arXiv:2005.13160 [astro-ph.GA] .
- [73] V. Ravi, M. Catha, L. D'Addario, *et al.*, *Nature (London)* **572**, 352 (2019), arXiv:1907.01542 [astro-ph.HE] .
- [74] J. S. Chittidi, S. Simha, A. Mannings, *et al.*, *Astrophys. J.* **922**, 173 (2021), arXiv:2005.13158 [astro-ph.GA] .
- [75] K. E. Heintz, J. X. Prochaska, S. Simha, *et al.*, *Astrophys. J.* **903**, 152 (2020), arXiv:2009.10747 [astro-ph.GA] .
- [76] C. J. Law, B. J. Butler, J. X. Prochaska, *et al.*, *Astrophys. J.* **899**, 161 (2020), arXiv:2007.02155 [astro-ph.HE] .
- [77] V. Ravi, C. J. Law, D. Li, *et al.*, *Mon. Not. R. Astron. Soc.* **513**, 982 (2022), arXiv:2106.09710 [astro-ph.HE] .
- [78] C. W. James, E. M. Ghosh, J. X. Prochaska, *et al.*, *Mon. Not. R. Astron. Soc.* **516**, 4862 (2022), arXiv:2208.00819 [astro-ph.CO] .
- [79] S. D. Ryder, K. W. Bannister, S. Bhandari, *et al.*, arXiv e-prints , arXiv:2210.04680 (2022), arXiv:2210.04680 [astro-ph.HE] .
- [80] D. Foreman-Mackey, D. W. Hogg, D. Lang, and J. Goodman, *Pub. Astro. Soc. Pacific* **125**, 306 (2013), arXiv:1202.3665 [astro-ph.IM] .